Cross density variation and vorticity generation in compressible shears

M. BELAN† - S. DE PONTE† - D. TORDELLA‡
†: Dipartimento di Ingegneria Aerospaziale - Politecnico di Milano
‡: Dipartimento di Ingegneria Aerospaziale - Politecnico di Torino

– M.Belan, S.De Ponte, S.Massaglia and D. Tordella "Experiments and numerical simulations on the mid-term evolution of hypersonic jets", *Astrophysics and Space Science*, 293 (1-2): 225-232, 2004

– M.Belan, S. Deponte, S.Massaglia and D. Tordella "Hypersonic Jet in the Laboratory", *Virtual Astrophysical Jets*, Dogliani, October 2nd-4th, 2003.

– S.Massaglia, M.Belan, S.De Ponte, D.Tordella, M.Iovieno, G.Bodo, A.Ferrari, P.Rossi, "Hypersonic Jets in the laboratory", *Jenam 2002 - 11th Meeting of the European Astronomical Society*, Porto, 2-7 Settembre 2002.

– Belan M., Tordella D., De Ponte S. "A system of fast acceleration of a mass of gas for the laboratory partial simulation of stellar jets", *The 19th ICIASF*, Cleveland, August 27-30, 2001.

– Belan M., De Ponte S., D'Ambrosio D., Tordella D. Design of an experiment on the spatial evolution of hypersonic jets. *XVI Congresso Nazionale Aidaa*, Palermo (Settembre 2001).

The lateral spreading of the compressible mixing layer is studied by means of the independent variation of two control parameters

The adjustable pressures (stagnation / ambient)

- control the Mach number of the underexpanded jets (quasi-stationary flows)

The indipendent selection of the jet gas and the medium gas

- set the density ratio $\rho_{\mathrm{jet}}/\rho_{\mathrm{amb}}$

The facility

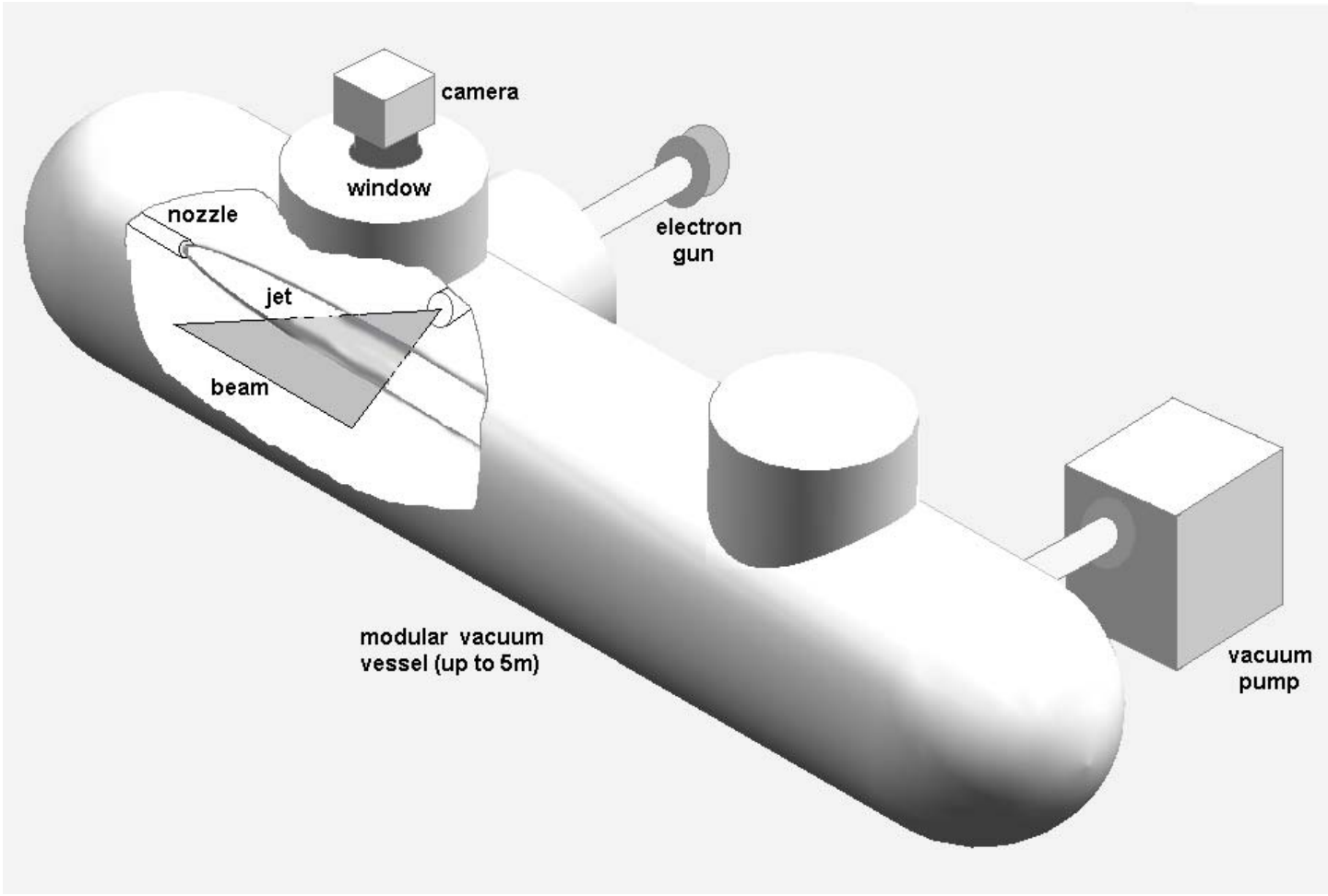

•Vacuum vessel •Nozzles •Electron gun •High-sensitivity camera

Capability of the system

- 2D Visualization of 3D flows (slices)
- Density measurements
- Concentration measurements
- mid-long term spatial evolution can be observed (up to 100 times the formation scale)

Laboratory / astrophysical jets: similitude

- Mach number $\mathcal{M}$
- Density ratio $\rho_{\text{jet}}/\rho_{\text{amb}}$.
- $Re_{\text{lab}} \ll Re_{\text{eff}}$ (small scale)
- $T_{\text{lab}} \ll T_{\text{eff}}$ (no heating at present)

Density measurements

Radiant intensity I vs numerical density n:

$$I = \frac{c\,n}{1 + \left(2\,n\,\sigma^2 {P_{mn}}^{-1} \sqrt{\frac{4\pi}{m} kT}\right)} = \frac{c_1\,n}{1 + c_2\,n}$$

Gadamer curve for electron beams:

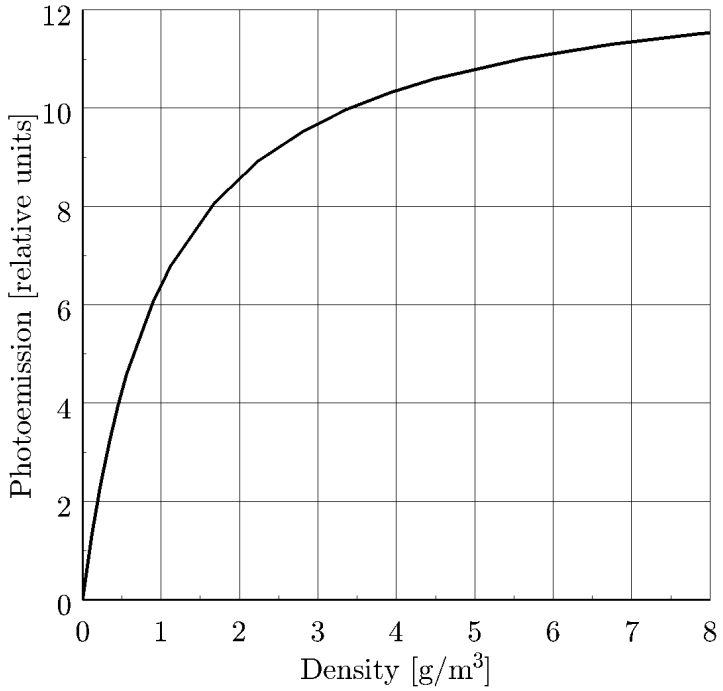

Intensity I vs density ρ:

$$I = \frac{c_1\,\rho}{1 + c_2\,\rho}; \qquad I \to I_{max} \text{ as } \rho \to \infty$$

- Linearity at low densities:
  $\rho \simeq I/c_1$
  (lower limit: CCD noise level)

- Saturation at high densities (physical limit): inverse function correction
  $\rho = I/(c_1 - c_2 I)$
  (upper limit: noise amplification, $\mathrm{d}\rho/\mathrm{dI} \to \infty$ as $I \to I_{max}$)

The underexpanded jets

U.e. jets

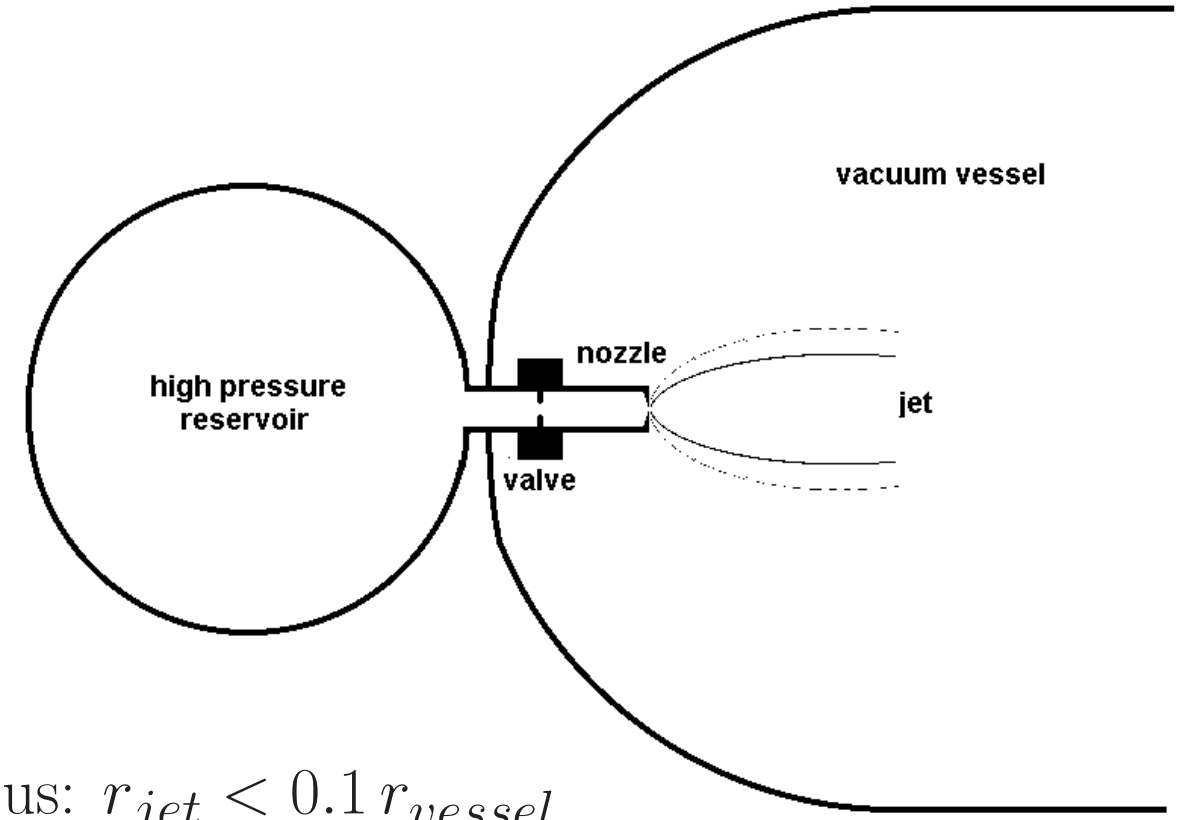

- Small jet radius: $r_{jet} < 0.1\, r_{vessel}$
- Quasi-stationary jet: $\Delta t_{valve} \gg t_{jet}$
- Mach number at the Mach disk up to 35.
- Stagnation/ambient density ratio: $\rho_o/\rho_{\mathrm{amb}}$ up to 10^5.
- Jet/ambient density ratio: $\rho_{\mathrm{jet}}/\rho_{\mathrm{amb}}$ from 0.2 to 8.

Jet structure:

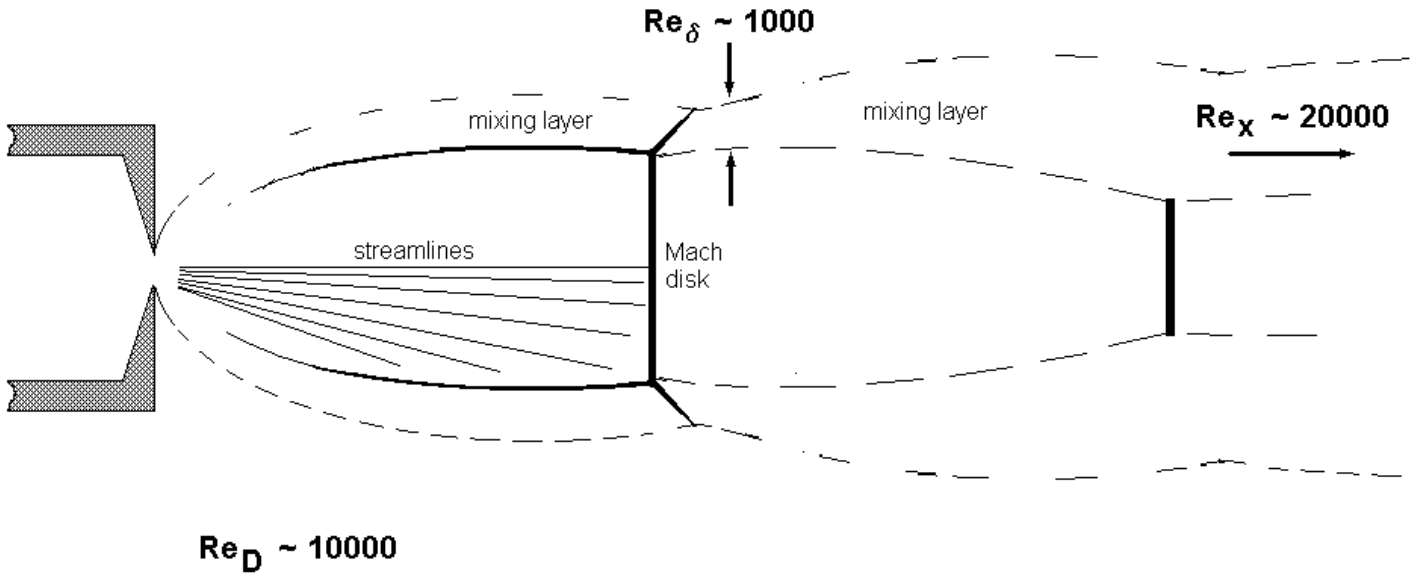

- nearly isoentropic flow on the axis up to the normal shock
- barrel shock, stationary
- Mach disk, stationary
- secondary shocks

Theoretical position z_m of the Mach disk: $\dfrac{z_m}{2\,r} = C_\gamma \sqrt{\dfrac{p_\mathrm{o}}{p_\mathrm{amb}}}$

Measurements range:
typical density curve along the axis

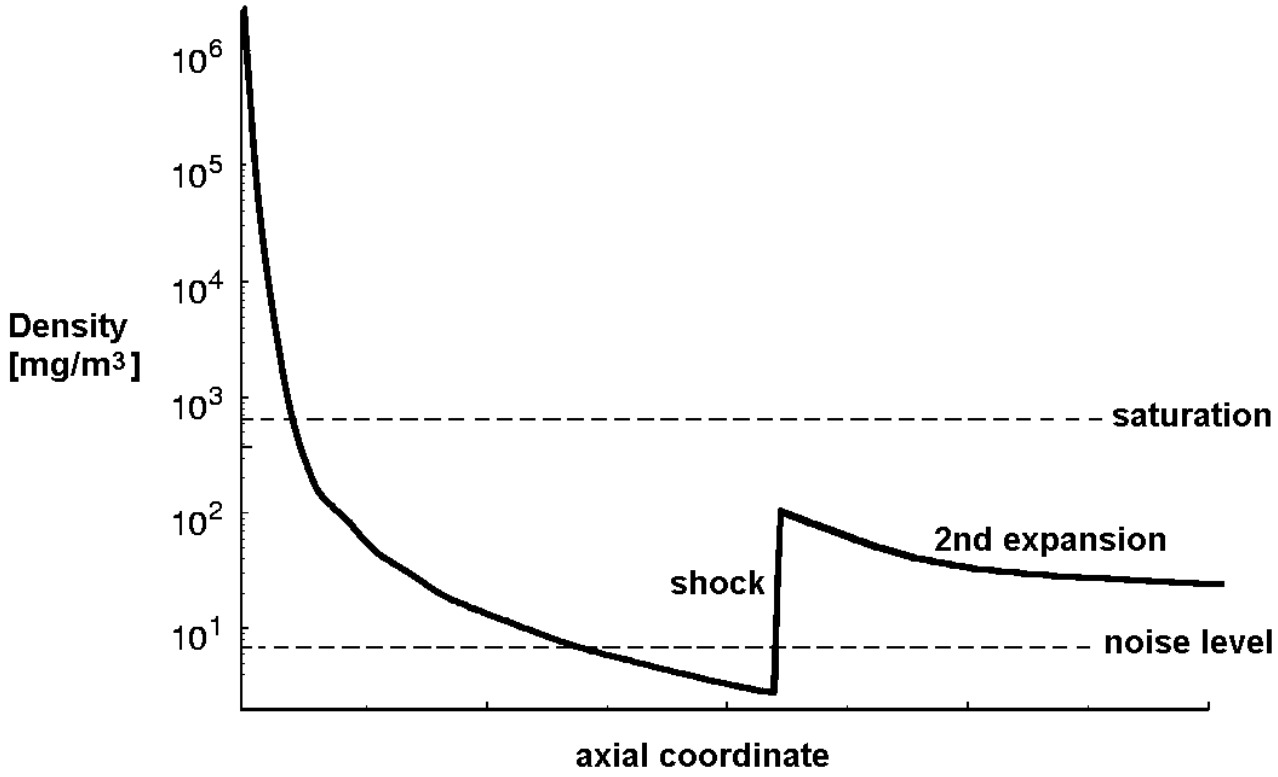

lower limit: noise – upper limit: saturation

Air jet in air medium

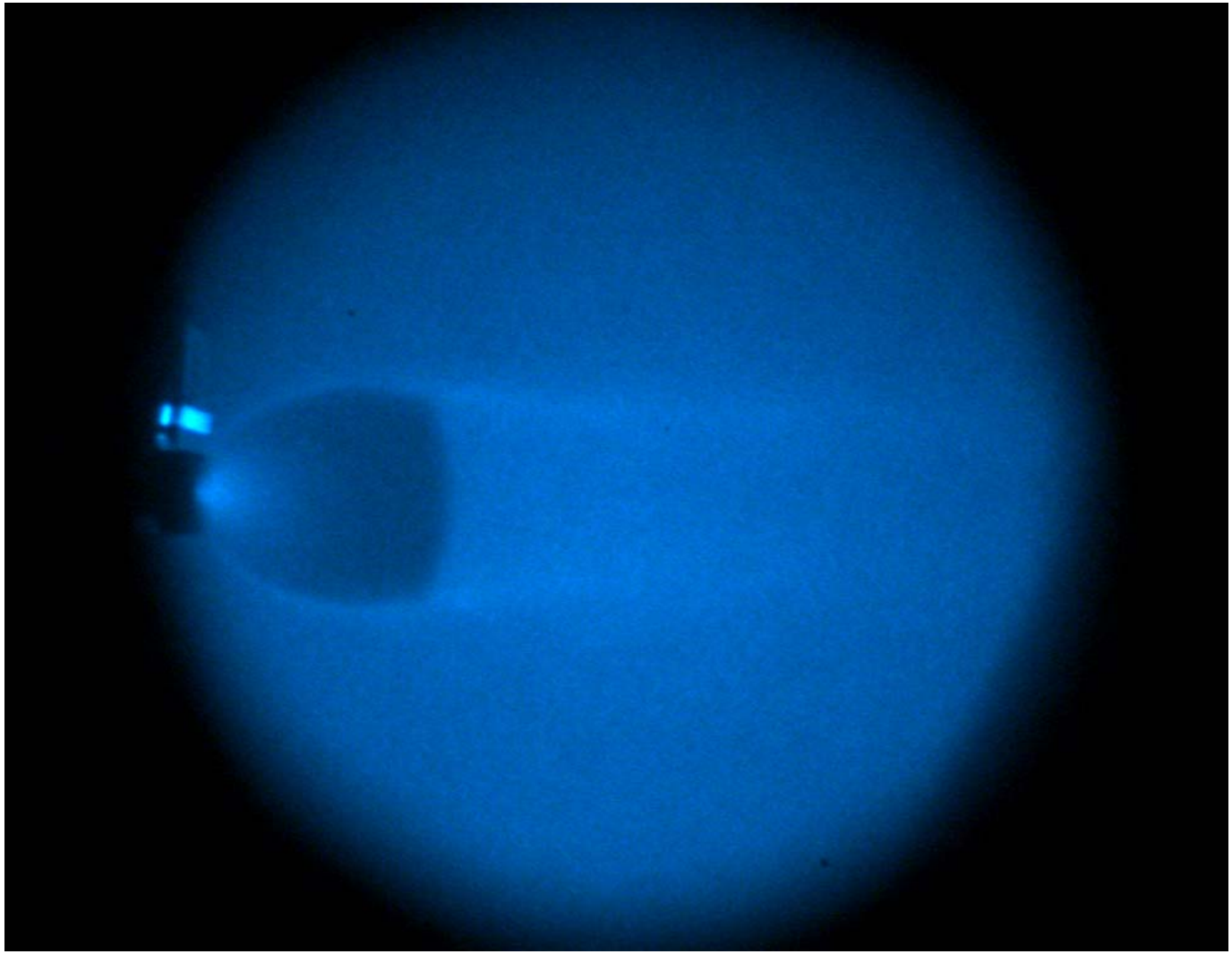

$\rho_{\mathrm{jet}}/\rho_{\mathrm{amb}} \simeq 1.1$; $M_{max} = 17$

Jet spreading visualization

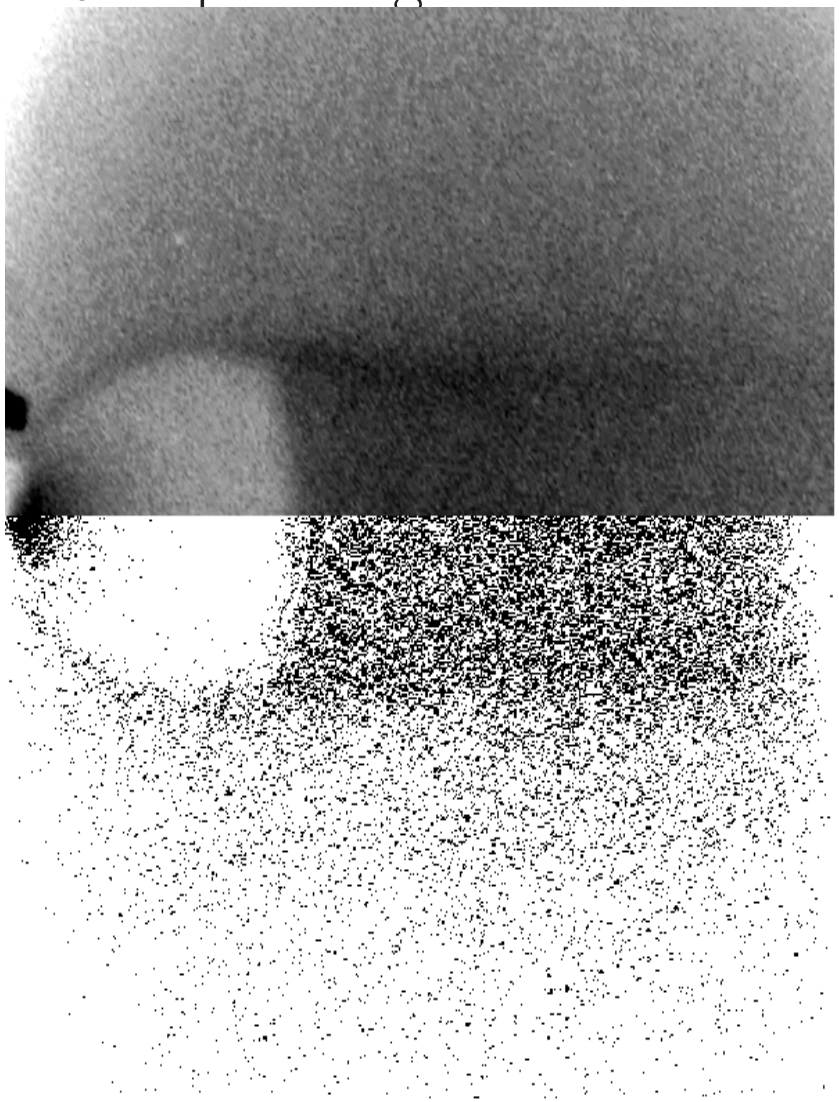

1D density map along the axis

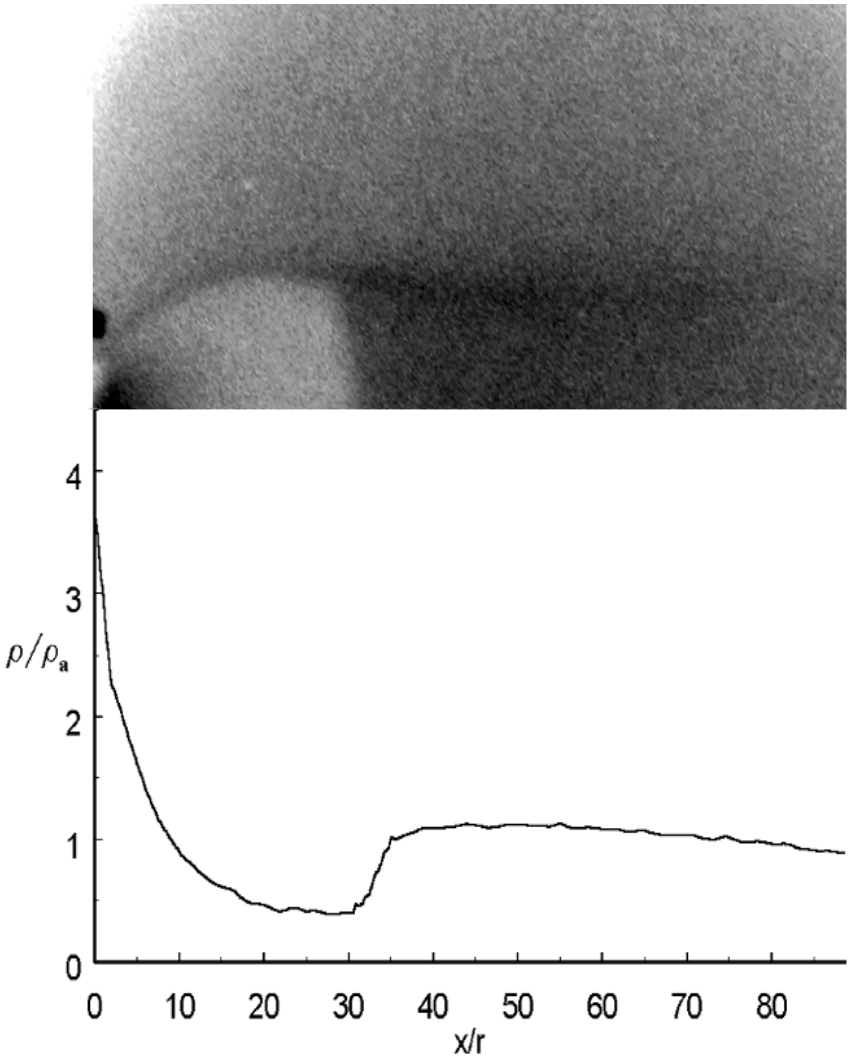

Air jet in helium medium

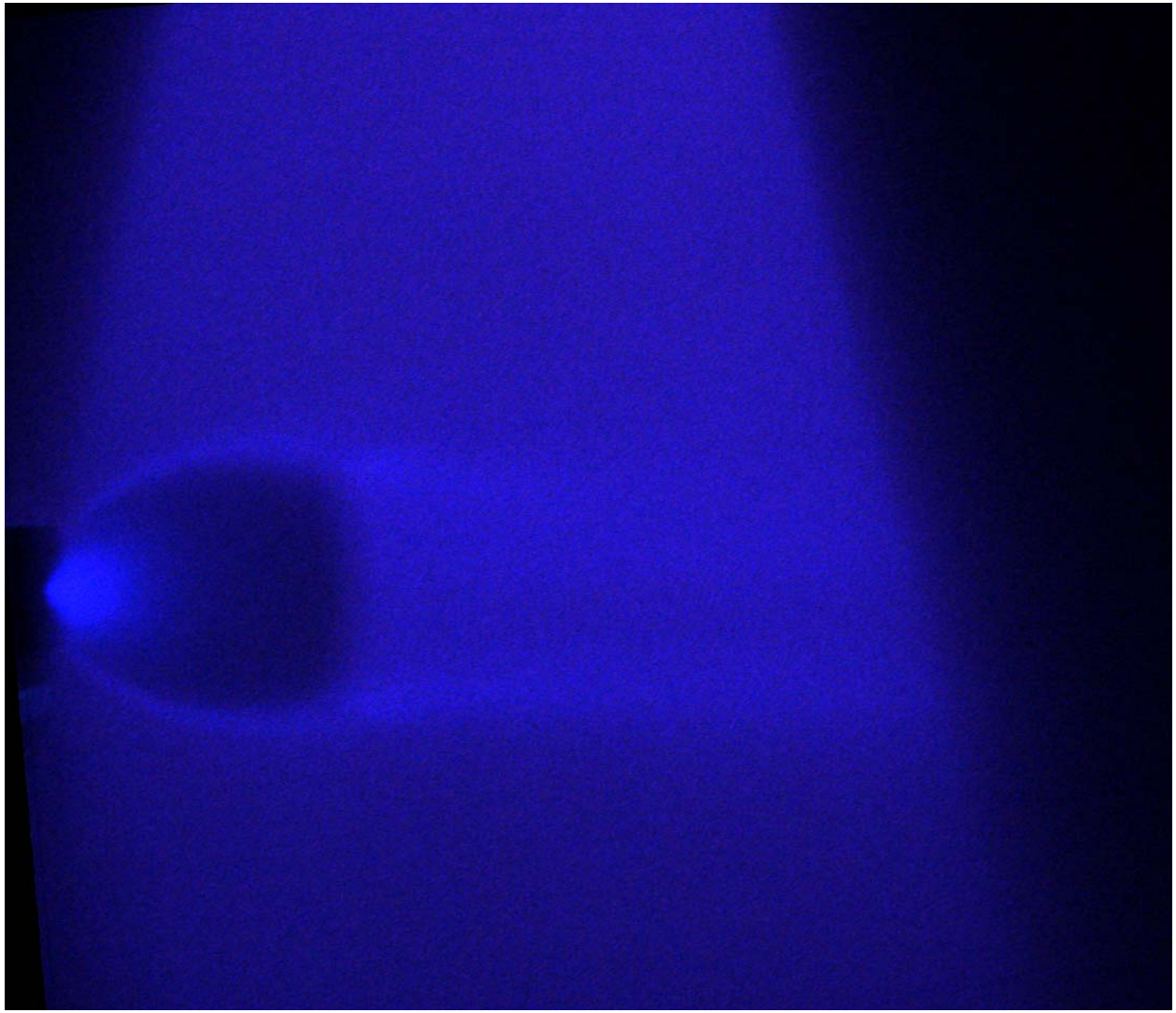

$\rho_{\mathrm{jet}}/\rho_{\mathrm{amb}} \simeq 8.0$; $M_{max} = 17$

Jet spreading visualizations (threshold images)

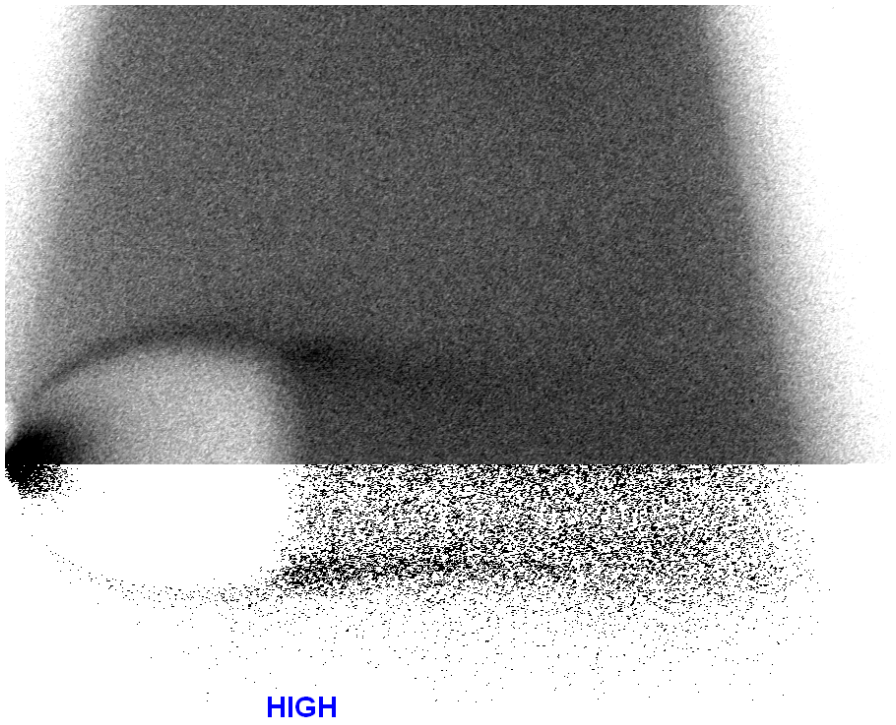

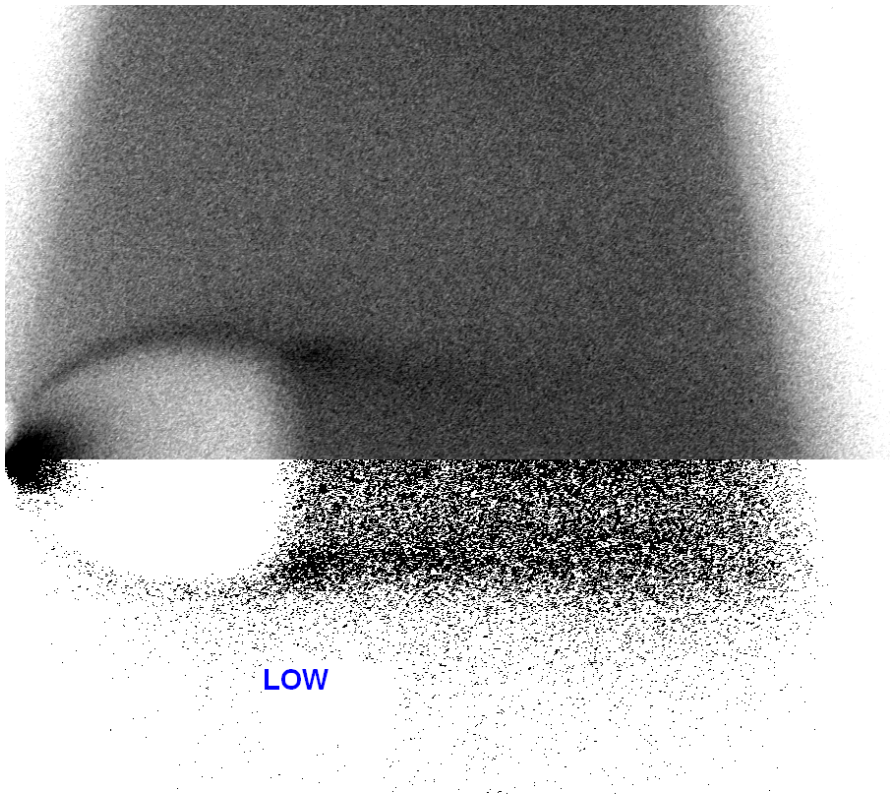

Helium jet in air medium

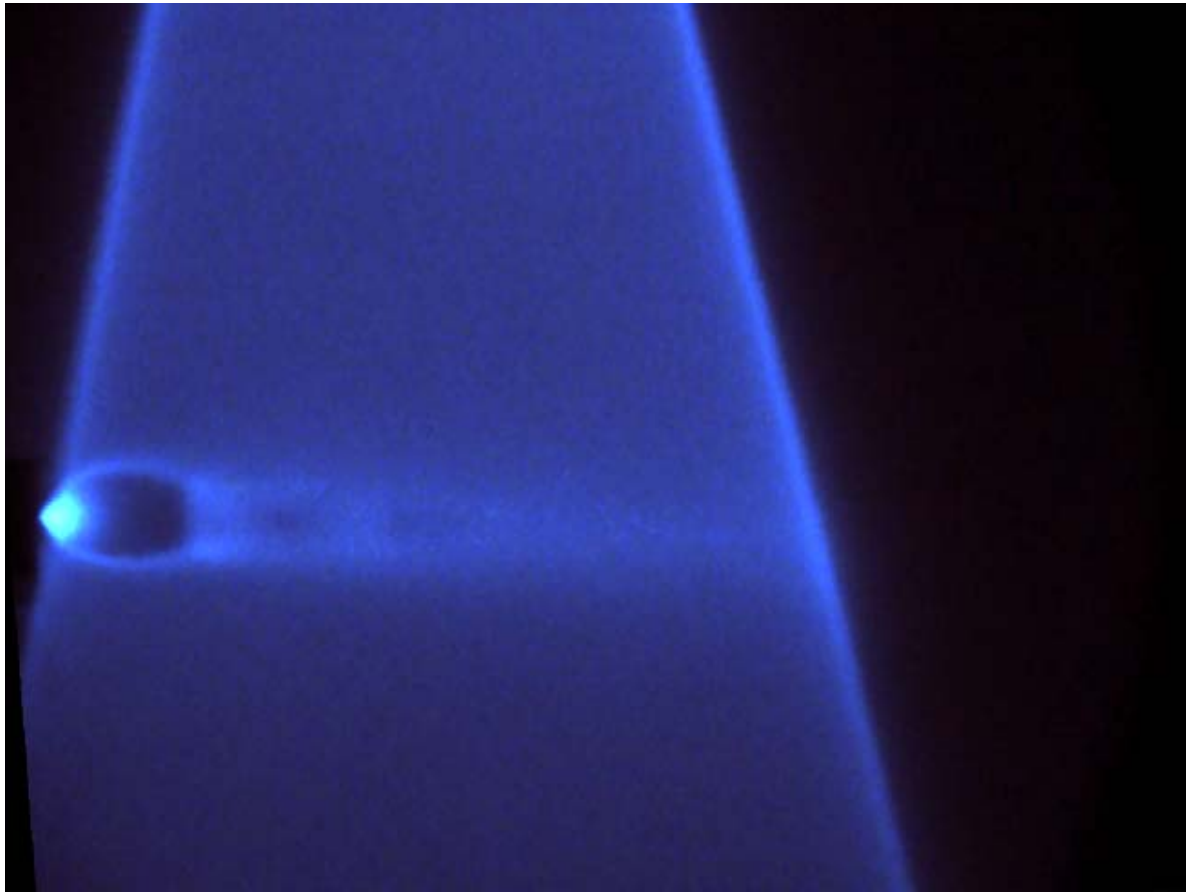

$\rho_{\mathrm{jet}}/\rho_{\mathrm{amb}} \simeq 0.2$; $M_{max} = 17$

Inner/outer jet spreading
(2-threshold image)

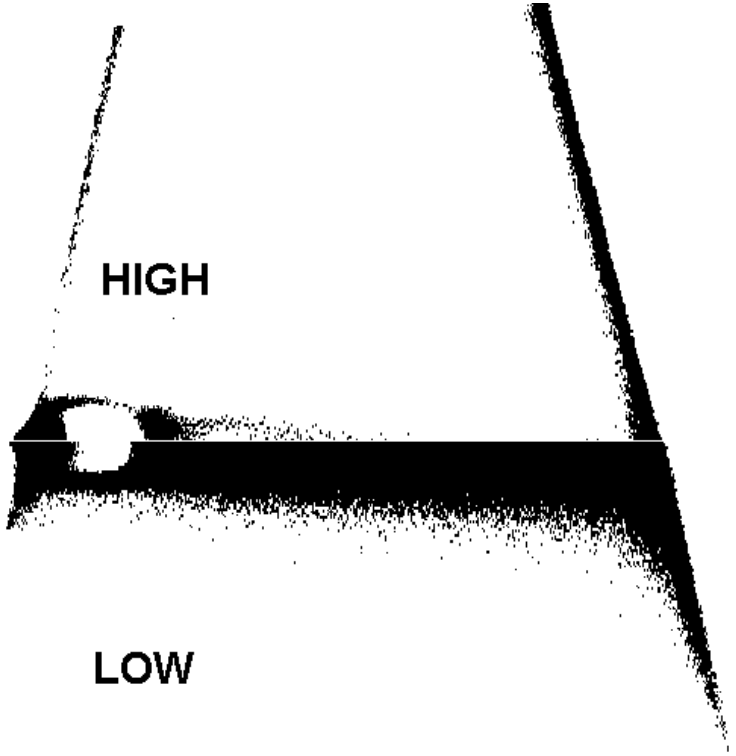

1D density map along the axis

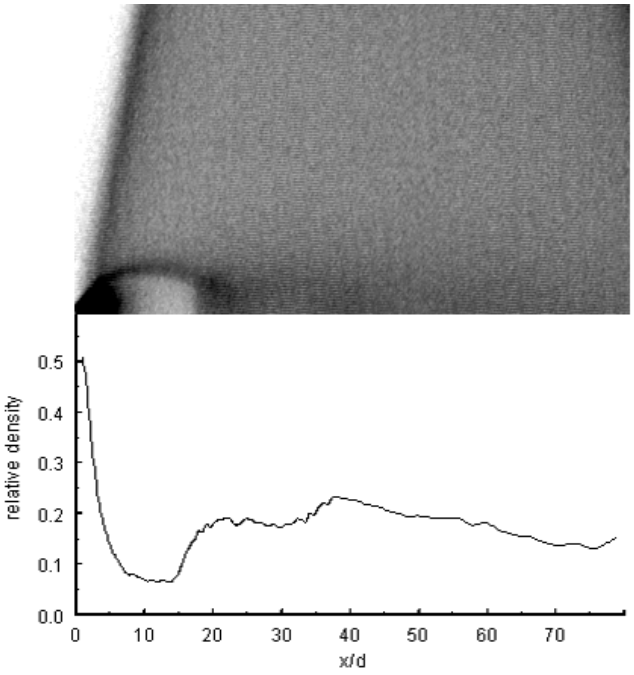

Helium jet in air medium

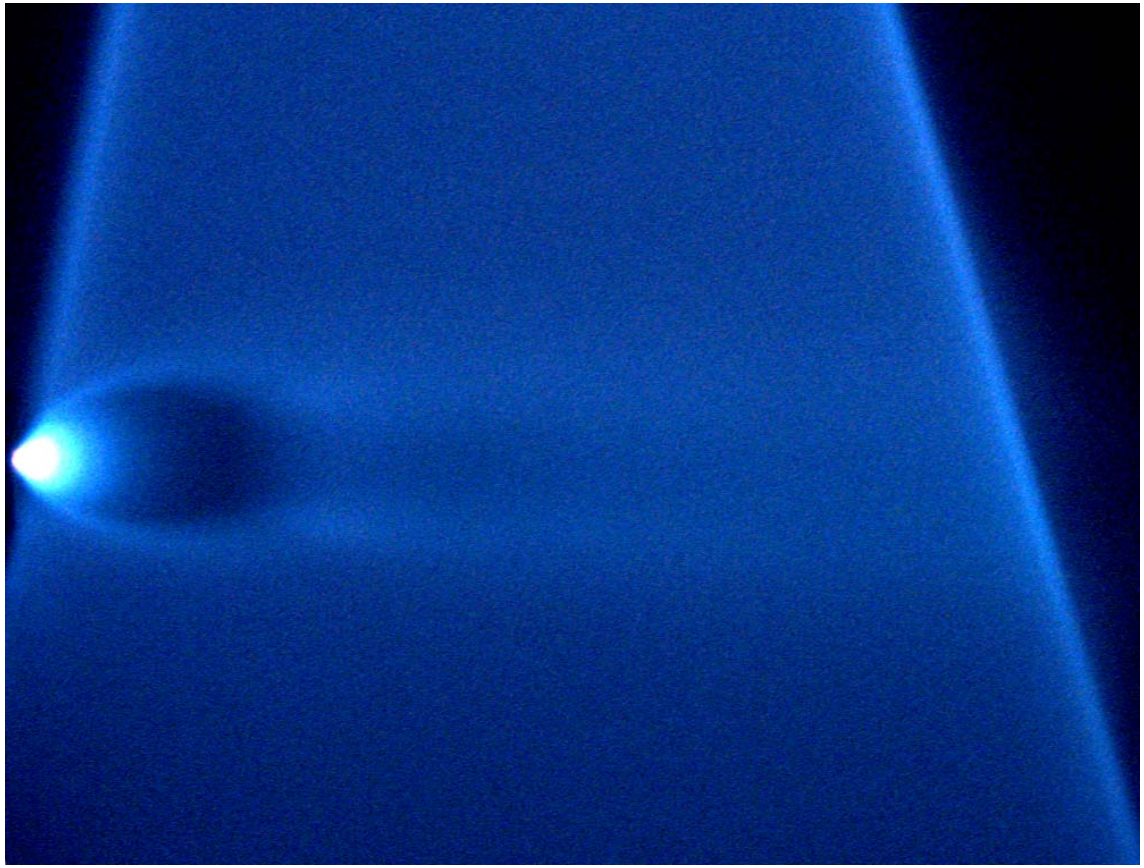

$\rho_{\mathrm{jet}}/\rho_{\mathrm{amb}} \simeq 0.2$; $M = 34$

Jet spreading visualization (threshold images)

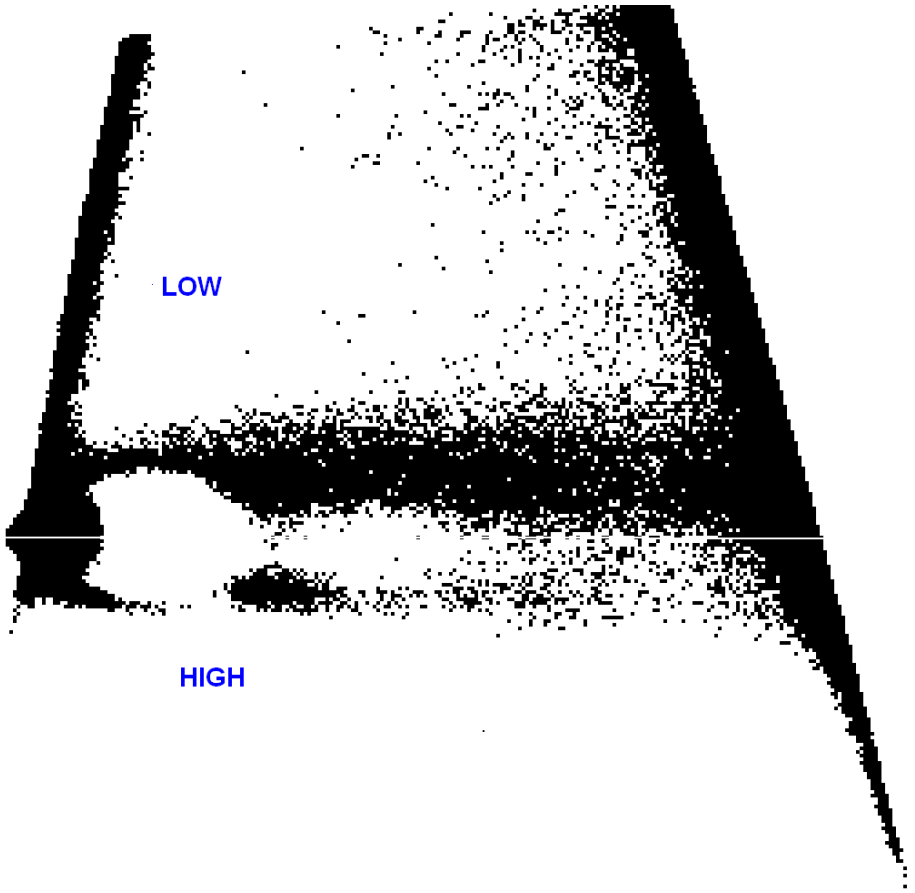

Vorticity and stability in the mixing layer

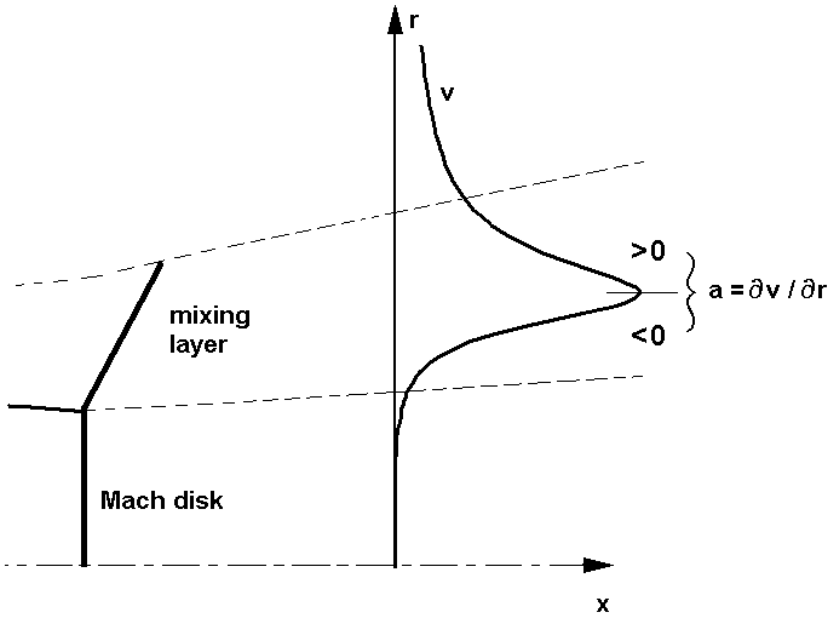

Lateral momentum distribution and entrainment from the ambient gas

$$\frac{D\omega}{Dt} \sim \frac{\nabla\rho}{\rho} \times (-a_r)$$

---

e.g. He in air $\nabla\rho \uparrow$: $a_r \uparrow$ $(-a_r \downarrow)$ INSTAB
$a_r \downarrow$ $(-a_r \uparrow)$ STAB

---

e.g. air in He $\nabla\rho \downarrow$: $a_r \uparrow$ $(-a_r \downarrow)$ STAB
$a_r \downarrow$ $(-a_r \uparrow)$ INSTAB

Conclusions

- By coupling the compressibility effect with the presence of density gradients associated to the ambient conditions (initial and lateral boundary conditions), it is observed that the lateral momentum distribution and the entrainment depend on the cross stream density variations.
- In particular, the spreading of the lateral mixing appears to be affected by the sign of the density differences:
- it is observed that if the density gradient is **concurrent** with the cross kinetic energy gradient the spreading is **lower** than if the density and energy gradient are **opposite**.

Other examples

Helium jet in air medium
adaptive threshold image (density gradients)

$\rho_{\mathrm{jet}}/\rho_{\mathrm{amb}} \simeq 0.2$; $M_{max} = 17$

Helium jet in air medium (collimated jets with multiple shocks)

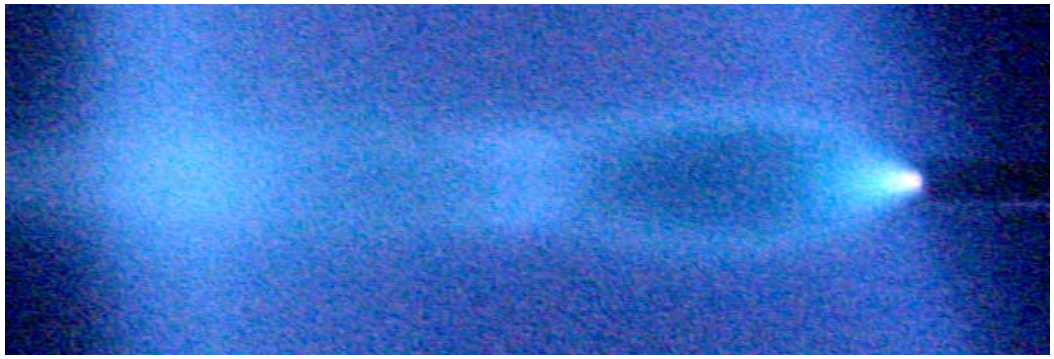

$\rho_{\rm jet}/\rho_{\rm amb} \simeq 0.05$, $M \simeq 28$ (behind the first shock)

$\rho_{\rm jet}/\rho_{\rm amb} \simeq 0.04$, $M \simeq 15$ (behind the first shock)

Argon jet in air medium

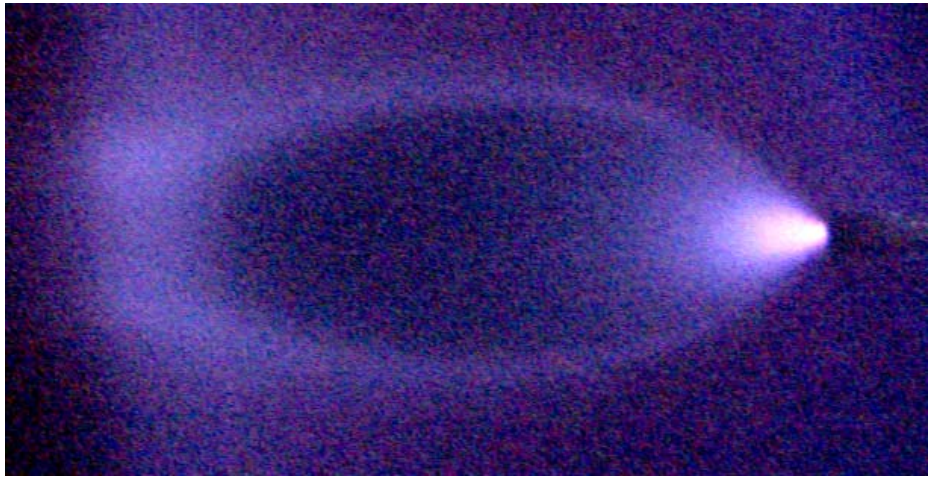

$$\rho_{\mathrm{jet}}/\rho_{\mathrm{amb}} \simeq 1$$
$$M > 30$$